Quaternion Unscented Kalman Filtering for Integrated Inertial Navigation and GPS

Wassim Khoder, Bienvenu Fassinut-Mombot, Mohammed Benjelloun
Laboratoire d'Analyse des Systèmes du Littoral, Université du Littoral Côte d'Opale

50 rue Ferdinand Buisson, BP 699, 62100 Calais, France
Email: {Wassim.Khoder,Bienvenu.Fassinut-Mombot,Mohammed.Benjelloun}@lasl-gw.univ-littoral.fr

Abstract—**In this paper, a Scaled Unscented Kalman Filter (SUKF) based on the quaternion concept is designed for integrating Inertial Navigation System (INS) aided by GPS measurements under large attitude error conditions. In this feedback filter, only the bias effects are considered to be independent states and are used to compensate for navigation errors. To preserve the nonlinear nature of the unit quaternion, the weighted mean computation for quaternions is derived in rotational space as a barycentric mean with renormalization and a multiplicative quaternion-error is used for predicted covariance computation of the quaternion because it represents the distance from the predicted mean quaternion. The updates are performed using quaternion multiplication which guarantees that quaternion normalization is maintained in the filter. Since the quaternion process noise increases the uncertainty in attitude orientation, modeling it as a rotation vector is considered. Simulation and experimental results indicate a satisfactory performance of the newly developed model.**

Keywords: Inertial Navigation System, Inertial sensor model, GPS, Quaternion attitude parameterization, Rotation vector, Scaled Augmented Unscented Kalman Filter (SUKF), Scaled Sigma Points.

I. Introduction

The principal software functions executed in the Inertial Navigation System (INS) computer are the angular rate signal into attitude integration function (denoted as attitude algorithms), use of the attitude data to transform measured acceleration signal into a suitable navigation coordinate frame where it is integrated into velocity and integration of the navigation frame velocity into position (denoted as velocity and position algorithms). Thus three integration functions (INS algorithm) are involved: attitude, velocity, and position, each of which requires high accuracy to assure negligible error compared to inertial sensors accuracy requirements.

Since acceleration from the accelerometers and angular rate from the rate gyros are generally susceptible to various measurement noise sources, the accuracy of position, velocity and attitude information degrades with time [1]–[4]. Recent research has shown that the growth of numerical errors in Inertial Measurement Units (IMUs) navigation with time can be prevented by using external aiding sensors such as the Global Positioning System (GPS) [5]–[7]. The benefits of this integration are well known. In this integration, the GPS receiver can provide various combinations of velocity-type and position-type measurements. As a result, the long-term INS errors are corrected by fusing IMU measurements with the GPS measurements, and the short-term faults of the GPS receiver can be effectively isolated by the INS. Since in INS algorithm, the accuracy of attitude information governs the accuracy of velocity and position estimation, the most researched topic for the INS integration functions has been primarily focused on the design of algorithms for the attitude integration function and initial alignment. Several parameterizations have been used to represent the attitude, such as Euler angles, Direct Cosine Matrix, Quaternions, Rotation vector, Rodrigues parameters, etc. The detailed discussion on each parametrization for attitude estimation is found in [7]–[9]. The Extended Kalman Filter (EKF) is widely used nonlinear filtering method for attitude estimation [10]. The Unscented Kalman Filter (UKF) is an extension of the classical Kalman filter to nonlinear process and measurement models and has been proposed for attitude estimation, which is more robust than the EKF for large initial attitude-error conditions [6], [9].

The quaternions method is advantageous since it requires less computation, gives better accuracy, avoids singularity and the kinematics equation is bilinear [11], [12]. However, the quaternion must obey a normalization constraint, which can be violated in many nonlinear quaternion filtering approaches. In fact, if the state vector is quaternion, the predicted quaternion mean should be calculated in the rotational space to preserve the nonlinear nature of unit quaternion.

To directly utilize UKF formulation built in vector space and to avoid a mean computation problem of quaternions, a modified method employing the combination of the quaternion with the generalized Rodrigues parameters is used in [7], [9]. This method converts a quaternion to a Rodrigues parameter and converted Rodrigues parameters are used to compute the predicted mean, the covariance and cross-relation matrix since Rodrigues parameters are unconstrained. Rodrigues parameters are converted back to quaternion because this method uses the inertial quaternion for state propagation. A UKF in a unit quaternion space is possible when a weighted mean of quaternions produces a unit quaternion estimate, and the predicted covariance computation and quaternion guarantees that quaternion in filter lies on unit sphere.

As an additional development, an alternative formulation for the square root version of the UKF is developed and presented in this paper for the integrated INS navigation and GPS.

This version is based on a generalized unconstrained three-component attitude-error vector to represent the quaternion error vector, where no parameter conversion is required, such as transformation between quaternions and Rodrigues parameters. A multiplicative quaternion-error is used for predicted covariance computation of the quaternion because it represents the distance from the predicted mean quaternion, and the unit quaternion is not closed for subtraction, guaranteeing that the quaternion in filter lies in unit quaternion space. The quaternion multiplication is used to perform the updates. Since quaternion process noise finally results in an increase of the uncertainty in attitude orientation, we treat then the quaternion error vector as a rotation vector. No small angle assumption is made in the model development.

II. Integration navigation dynamic model

This section defines the coordinate frames used in this paper and the concepts of quaternion. A summary of attitude quaternion, velocity and position dynamic models, the inertial sensor dynamic model and sensor error model compensation.

A. Coordinate systems

The coordinate systems used in this paper are inertial frame (i-frame), Earth-fixed frame (e-frame), navigational frame (n-frame), and body frame (b-frame).

The i-frame is fixed with the centre of the Earth as the origin and axes which are non-rotating with respect to the fixed stars with its x-axis points toward the vernal equinox direction (also known as the First Point of Aries or the vernal equinox point), the z-axis axis points in the direction of the North pole and the y-axis completes the right-handed system (note that the x-axis and y-axis are on the equator, which is the fundamental plane).

The e-frame coincides with the i-frame at the origin and z-axis but rotates with the Earth rate; however, the x-axis points in the direction of the Earth's prime meridian, and the y-axis completes the right-handed orthogonal frame.

The n-frame is used for local navigation purposes. It is formed by fitting a tangent plane to the geodetic reference ellipse at a point of interest. Axes of the n-frame is point in the directions north, east, down in that order. The benefit of the east-north-up (ENU) system is that altitude increases in the upward. The advantages of NED system are that the direction of a right turn is in the positive direction with respect to a downward axis, and the axes coincide with vehicle-fixed roll-pitch-heading coordinates when the vehicle is level and headed north [1].

The b-frame is an orthogonal axis set which is fixed onto the vehicle body and rotates with it. Conventions typically depend on the particular vehicle.

B. Attitude quaternion dynamic model

In order to determine the current attitude, we need an attitude evolution equation. Depending on which parameter set is used to express attitude, the attitude equation varies in forms. One of the most useful attitude parameterization is given by the quaternion, which is four-dimensional vector, defined as $\mathbf{q} \equiv [\varrho^T \ \mathbf{q}_4]^T$, with $\varrho \equiv [\mathbf{q}_1 \ \mathbf{q}_2 \ \mathbf{q}_3]^T$ is the vector part and $\mathbf{q}_4$ the real part of quaternion. The quaternion satisfies the following normalization constraint given by

$$\mathbf{q}^T\mathbf{q} = \|\mathbf{q}\|^2 = \varrho^T\varrho + \mathbf{q}_4^2 = 1 \tag{1}$$

The attitude matrix that transform the north-east-down (NED) frame, n-frame, to the body frame, b-frame is related to the quaternion by [13]

$$\mathbf{C}_n^b(\mathbf{q}) = (\mathbf{q}_4^2 - \varrho^T\varrho)\mathbf{I}_{3\times3} + 2\varrho\varrho^T - 2\mathbf{q}_4\langle\varrho\times\rangle \tag{2a}$$

$$= \Xi^T(\mathbf{q})\Psi(\mathbf{q}) \tag{2b}$$

where $\mathbf{I}_{3\times3}$ is a 3×3 identity matrix and

$$\Xi(\mathbf{q}) \equiv \begin{bmatrix} \langle\varrho\times\rangle + \mathbf{q}_4\mathbf{I}_{3\times3} \\ -\varrho^T \end{bmatrix}, \quad \Psi(\mathbf{q}) \equiv \begin{bmatrix} -\langle\varrho\times\rangle + \mathbf{q}_4\mathbf{I}_{3\times3} \\ -\varrho^T \end{bmatrix} \tag{3}$$

also, $\langle\varrho\times\rangle$ denotes the cross-product matrix that is associated with ϱ, and that is defined as follows:

$$\langle\varrho\times\rangle \equiv \begin{bmatrix} 0 & -\mathbf{q}_3 & \mathbf{q}_2 \\ \mathbf{q}_3 & 0 & -\mathbf{q}_1 \\ -\mathbf{q}_2 & \mathbf{q}_1 & 0 \end{bmatrix} \tag{4}$$

An advantage to using quaternions is that the attitude matrix is quadratic in the parameters and also does not involve transcendental functions.

The attitude quaternion dynamic equation is given by

$$\dot{\mathbf{q}} = \frac{1}{2}\Omega_{nb}^{*b}\mathbf{q} = \frac{1}{2}\Xi(\mathbf{q})\omega_{nb}^b \tag{5}$$

where the 4×4 matrix Ω_{nb}^{*b} is a function of ω_{nb}^b which is the rotation rate between the n-frame and the b-frame solved in the b-frame. This function is presented by

$$\Omega_{nb}^{*b} \equiv \begin{bmatrix} -\langle\omega_{nb}^b\times\rangle & \omega_{nb}^b \\ -(\omega_{nb}^b)^T & 0 \end{bmatrix} \tag{6}$$

A major advantage of using quaternions is that the kinematics equation is linear in the quaternion and is also free of singularities. Another advantage of quaternions is that successive rotations can be accomplished using quaternion multiplication. This can be written using $\mathbf{C}(\mathbf{q}')\mathbf{C}(\mathbf{q}) = \mathbf{C}(\mathbf{q}' \otimes \mathbf{q})$. The composition of the quaternions is bilinear, with $\mathbf{q}' \otimes \mathbf{q} = [\Psi(\mathbf{q}') \ \mathbf{q}']\mathbf{q} = [\Xi(\mathbf{q}) \ \mathbf{q}]\mathbf{q}'$. Also, the inverse quaternion is defined by $\mathbf{q}^{-1} \equiv [-\varrho^T \ \mathbf{q}_4]^T$ Note that $\mathbf{q} \otimes \mathbf{q}^{-1} = [0\ 0\ 0\ 1]^T$, which is the identity quaternion.

Remark that Eq. (5) cannot be used directly with the gyro measurement. However, this problem can be overcome by using the following identity:

$$\omega_{ib}^b = \omega_{in}^b + \omega_{nb}^b \tag{7}$$

Solving Eq. (7) for ω_{nb}^b and substituting $\omega_{in}^b = \mathbf{C}_n^b(\mathbf{q})\omega_{in}^n$ yields

$$\omega_{nb}^{b} = \omega_{ib}^{b} - \mathbf{C}_{n}^{b}(\mathbf{q})\omega_{in}^{n} \tag{8}$$

where

$$\omega_{in}^{n} = \omega_{ie}^{n} + \omega_{en}^{n} = \omega_{e}\begin{bmatrix} \cos\varphi \\ 0 \\ -\sin\varphi \end{bmatrix} + \begin{bmatrix} \left(\dfrac{v_E}{R_n + h}\right) \\ \left(-\dfrac{v_N}{R_m + h}\right) \\ \left(-\dfrac{v_E \tan\varphi}{R_n + h}\right) \end{bmatrix} \tag{9}$$

with φ represents latitude, λ represents longitude, v_N, v_E are velocity components in the north and east direction, respectively; ω_e is the magnitude of the Earth's rotation rate and $R_m = R_e(1-e^2)/(1-e^2\sin^2\varphi)^{3/2}$, $R_n = R_e(1-e^2\sin^2\varphi)^{1/2}$ are radii of curvature in the meridian and prime vertical, respectively, R_e is the radius of the Earth at the equator and e represents linear eccentricity of the reference ellipsoid.

C. Velocity and Position dynamic model

This means that the accelerometer measurements or specific forces from the accelerometer triad are obtained in the body frame, hence they need to be transformed to the navigation frame in order to be used in the navigation equation

$$\mathbf{f}^{n} \equiv \begin{bmatrix} f_N \\ f_E \\ f_D \end{bmatrix} = \mathbf{q} \otimes \mathbf{f}^{b} \otimes \mathbf{q}^{-1} = \mathbf{C}_{b}^{n}(\mathbf{q})\mathbf{f}^{b} \tag{10}$$

where $\mathbf{C}_{b}^{n}(\mathbf{q})$ is the attitude-quaternion matrix transpose of $\mathbf{C}_{n}^{b}(\mathbf{q})$. Then the velocity navigation equation that derived by the Coriolis equation [4], becomes

$$\dot{\mathbf{v}}^{n} = \mathbf{C}_{b}^{n}(\mathbf{q})\mathbf{f}^{b} + \mathbf{g}^{n} - \langle(2\omega_{ie}^{n} + \omega_{in}^{n})\times\rangle\,\mathbf{v}^{n} \tag{11}$$

where $\mathbf{v}^n$ is the velocity of the vehicle represented in the n-frame, $\mathbf{g}^n$ is the gravitational force represented in the n-frame, $\mathbf{f}^b$ represents specific force measured at the accelerometer, ω_{xy}^{z} is angular velocity of the y-frame relative to the x-frame expressed in z-frame coordinates, and Ω_{xy}^{z} denotes a skew-symmetric matrix function which represents the cross product $\langle\omega_{xy}^{z} \times (\cdot)\rangle = \langle\omega_{xy}^{z}\times\rangle(\cdot)$.

The INS computes position vector by integrating velocity vector. Therefore, the $\mathbf{C}_{e}^{n}(\mathbf{q})$ attitude-quaternion matrix defining the angular orientation between the e-frame and the n-frame, contains information about the geodetic coordinates φ and λ, latitude and longitude, respectively [4], [14], [15]. Then, the position evolution can be expressed as the following quaternion differential equation in NED coordinates

$$\dot{\mathbf{C}}_{e}^{n}(\mathbf{q}) = -\Omega_{en}^{n}\mathbf{C}_{e}^{n}(\mathbf{q}), \quad \dot{h} = \mathbf{u}_{zn}^{n}\mathbf{v}^{n} \tag{12}$$

where h is altitude above the Earth (height), $\mathbf{u}_{zn}^{n}$ is unit vector upward along the geodetic vertical (the z axis of the n-frame).

D. Inertial Sensor dynamic model

The inertial sensors measure rotation rates around three orthogonal axes and linear acceleration along three orthogonal axes using three axis gyros and three accelerometers to make a complete six degree-of-freedom measurement of the dynamics. The angular rate and specific force measured by the gyro and accelerometer respectively can be expressed in the simplified forms:

$$\widetilde{\omega}_{ib}^{b} = (\mathbf{I}_{3\times3} + \Gamma_{g}(\mathbf{SF},\mathbf{MA}))\omega_{ib}^{b} + \mathbf{b}_{g} + \eta_{g} \tag{13a}$$

$$\widetilde{\mathbf{f}}^{b} = (\mathbf{I}_{3\times3} + \Gamma_{a}(\mathbf{SF},\mathbf{MA}))\mathbf{f}^{b} + \mathbf{b}_{a} + \eta_{a} \tag{13b}$$

where $\widetilde{\omega}_{ib}^{b}$, $\widetilde{\mathbf{f}}^{b}$ represent the measured angular rate and specific force, respectively. ω_{ib}^{b}, $\mathbf{f}^{b}$ represent the true angular rate and the true specific force, respectively. $\mathbf{b}_a$, $\mathbf{b}_g$ represent the gyro and the accelerometer biases, respectively. η_g, η_a represent the gyro and the accelerometer measurement noises and the subscripts 'a' and 'g' represent the accelerometer and gyroscope triads, respectively. $\Gamma_g(\mathbf{SF},\mathbf{MA})$, $\Gamma_a(\mathbf{SF},\mathbf{MA})$ are the 3×3 dimensional matrices of gyro and accelerometer scale factors/misalignments (non-orthogonalities) errors, and are defined as follows:

$$\Gamma_{(\cdot)}(\mathbf{SF},\mathbf{MA}) = \begin{bmatrix} \mathbf{SF}_x & \mathbf{MA}_{xy} & \mathbf{MA}_{xz} \\ \mathbf{MA}_{yx} & \mathbf{SF}_y & \mathbf{MA}_{yz} \\ \mathbf{MA}_{zx} & \mathbf{MA}_{zy} & \mathbf{SF}_z \end{bmatrix} \tag{14}$$

where $\mathbf{SF}_x$, $\mathbf{SF}_y$, $\mathbf{SF}_z$ are the components of diagonal scale factor matrix $\mathbf{SF}$ and $\mathbf{MA}_{xy}$, $\mathbf{MA}_{xz}$, $\mathbf{MA}_{yx}$, $\mathbf{MA}_{yz}$, $\mathbf{MA}_{zx}$, $\mathbf{MA}_{zy}$ are the components of misalignment matrix $\mathbf{MA}$.

Simulating gyro and accelerometer using computers is not easy since continuous measurements cannot be generated using digital computers. Also, The outputs of the inertial sensors are the incremental angles $\Delta\widetilde{\theta}_k$ due to angular rate $\widetilde{\omega}_{ib}^{b}$ and incremental velocities $\Delta\widetilde{\mathbf{v}}_{\mathbf{f}k}^{b}$ due to the specific force $\widetilde{\mathbf{f}}^{b}$, and are obtained by integrating Eqs. (13a) and (13b), respectively, as follows:

$$\Delta\widetilde{\theta}_k = \int_{t_{k-1}}^{t_k} \widetilde{\omega}_{ib}^{b}(t)dt, \quad \Delta\widetilde{\mathbf{v}}_{\mathbf{f}k}^{b} = \int_{t_{k-1}}^{t_k} \widetilde{\mathbf{f}}^{b}(t)dt \tag{15}$$

E. Navigation error model compensation

In the feedback method developed in this paper, only inertial sensor error estimates from the INS filter algorithm are used to compensate for navigation errors. Then, the compensation inertial sensor measurement is accomplished rewritten the Eq. (15) to express true integrated inertial sensor measurement, as follows [6]:

$$\Delta\theta_k = \left[\mathbf{I} + \Gamma_{g}^{0}(\mathbf{SF},\mathbf{MA}) + \Gamma_{gk}(\mathbf{SF},\mathbf{MA})\right]^{-1} \left[\Delta\widetilde{\theta}_k - (\mathbf{b}_{g}^{0} + \mathbf{b}_{gk})\Delta t_k - \eta_{g(k-1)}\right] \tag{16a}$$

$$\Delta\mathbf{v}_{\mathbf{f}k}^{b} = \left[\mathbf{I} + \Gamma_{a}^{0}(\mathbf{SF},\mathbf{MA}) + \Gamma_{ak}(\mathbf{SF},\mathbf{MA})\right]^{-1} \left[\Delta\widetilde{\mathbf{v}}_{\mathbf{f}k}^{b} - (\mathbf{b}_{a}^{0} + \mathbf{b}_{ak})\Delta t_k - \eta_{a(k-1)}\right] \tag{16b}$$

where $\Delta\theta_k$ and $\Delta\mathbf{v}_{\mathbf{f}k}^b$ are the compensated outputs of the gyro and the accelerometer, respectively. $\Delta t_k = t_k - t_{k-1}$ is the incremental time interval between two successive measurements at t_k and t_{k-1}. The superscript '0' represents known quantities.

The discrete-time sensor error model can be applied as follows [6]:

$$\mathbf{b}_k = diag(\mathbf{d_b})\mathbf{b}_{k-1} + \eta_{\mathbf{b}_{k-1}} \tag{17a}$$

$$\mathbf{SF}_k = diag(\mathbf{d_{SF}})\mathbf{SF}_{k-1} + \eta_{\mathbf{SF}_{k-1}} \tag{17b}$$

$$\mathbf{MA}_k = diag(\mathbf{d_{MA}})\mathbf{MA}_{k-1} + \eta_{\mathbf{MA}_{k-1}} \tag{17c}$$

where $\mathbf{d_b}$, $\mathbf{d_{SF}}$, $\mathbf{d_{MA}}$, $\eta_\mathbf{b}$, $\eta_\mathbf{SF}$ and $\eta_\mathbf{MA}$ are discrete-time sensor error model parameters that can represent the random walk, the random constant and the first-order Gauss-Markov processes.

III. The Quaternion Scaled Unscented Kalman Filter (Q-SUKF)

In order to fuse aiding GPS measurements with the INS navigation algorithm to guarantee the accuracy of attitude information, the Unscented Kalman Filter (UKF) based on a quaternion parametrization is used. A description of the UKF can be found in [16]–[18]. The UKF is based on the unscented transformation which is referred to the procedure of obtaining a set of deterministically chosen points, called the sigma points, to represent the untransformed mean and covariance of the variable to be estimated [19]. By choosing appropriate weights, which obey the constraint that the sum of the weights is equal to 1, the weighted average and the weighted outer product of the transformed points give the mean and covariance of the transformed distribution. This is true when the state vector elements lie in a vector space. However, if the state vector is quaternion, the predicted quaternion mean should be calculated in the rotational space to preserve the nonlinear nature of unit quaternion. The straightforward implementation of the UKF with quaternions is possible when a weighted mean of quaternions produces a unit quaternion estimate, and the predicted covariance computation and quaternion guarantees that quaternion in filter lies on unit sphere.

Generally, the number of sigma points is $(2p+1)$ (augmented state dimension p). However, in the reduced sigma point filter, a set of $(p+2)$ sigma points can be constructed that fully captures all of the known statistics of the distribution [18]. In this paper the spherical simplex scaled sigma points are utilized to implement the UKF with quaternions because it generates better numerical properties [20], [21].

Let us consider the general nonlinear system process and measurement dynamic models:

$$\mathbf{x}_{k+1} \equiv \mathbf{g}[t_k, \mathbf{x}_k, \eta_{\mathbf{x}k}, \mathbf{u}_k], \qquad \Sigma_{\mathbf{x}k} = E[\eta_{\mathbf{x}k}\eta_{\mathbf{x}k}^T] \tag{18a}$$

$$\mathbf{z}_k \equiv \mathbf{h}[t_k, \mathbf{x}_k, \eta_{\mathbf{z}_k}], \qquad \Sigma_{\mathbf{z}k} = E[\eta_{\mathbf{z}k}\eta_{\mathbf{z}k}^T] \tag{18b}$$

where $\mathbf{x}_k$, $\mathbf{u}_k$ and $\mathbf{z}_k$ are the state, input and outputs vectors at time t_k and $\eta_{\mathbf{x}k}$ and $\eta_{\mathbf{z}k}$ are the system process and measurement noises. The system process state and noise components together, $\mathbf{x}_k$ and $\eta_{\mathbf{x}k}$ and $\eta_{\mathbf{z}k}$, respectively, are concatenated to create the augmented state vector, $\mathbf{x}_k^\mathrm{a}$. So that the effect of process and measurement noises can be used to better capture the odd-order moment information. Note that $\Sigma_{\mathbf{x}k}$ and $\Sigma_{\mathbf{z}k}$ are the process and measurement general noise covariance matrices, respectively.

We begin by defining the following state vector, where the superscript '+' denotes an update:

$$\begin{aligned}\hat{\mathbf{x}}_k^+ \equiv \big[&(\hat{\mathbf{q}}_k^+)^T\ (\hat{\mathbf{p}}_k^+)^T\ (\hat{\mathbf{v}}_k^{n+})^T \\ &(\hat{\mathbf{b}}_{g_k}^+)^T\ (\hat{\mathbf{b}}_{a_k}^+)^T\ (\hat{\mathbf{SF}}_{g_k}^+)^T\ (\hat{\mathbf{SF}}_{a_k}^+)^T\ (\hat{\mathbf{MA}}_{g_k}^+)^T\ (\hat{\mathbf{MA}}_{a_k}^+)^T\big]\end{aligned} \tag{19}$$

where $\hat{\mathbf{q}}_k^+$ is the estimated quaternion, $\hat{\mathbf{p}}_k^+$ is the estimated position consisting of the latitude, φ, longitude, λ, and altitude, h, $\hat{\mathbf{v}}_k^{n+}$ is the estimated velocity vector, $\hat{\mathbf{b}}_{g_k}^+$ and $\hat{\mathbf{b}}_{a_k}^+$ are the estimated gyro and accelerometer biases, respectively, $\hat{\mathbf{SF}}_{g_k}^+$ and $\hat{\mathbf{SF}}_{a_k}^+$ are the the estimated gyro and accelerometer scale factors, respectively, and $\hat{\mathbf{MA}}_{g_k}^+$ and $\hat{\mathbf{MA}}_{a_k}^+$ are the the estimated gyro and accelerometer misalignments, respectively.

The first step is initialization of the augmented state $\hat{\mathbf{x}}_0^\mathrm{a}$ and augmented state error covariance $\mathbf{P}_0^{\mathrm{a}+}$ as follows:

$$\hat{\mathbf{x}}_0^{\mathrm{a}+} = \begin{bmatrix} \hat{\mathbf{x}}_0^+ \\ \mathbf{0} \\ \mathbf{0} \end{bmatrix}, \quad \mathbf{P}_0^{\mathrm{a}+} = \begin{bmatrix} \mathbf{P}_0^+ & \mathbf{0} & \mathbf{0} \\ \mathbf{0} & \Sigma_{\mathbf{x}0} & \mathbf{0} \\ \mathbf{0} & \mathbf{0} & \Sigma_{\mathbf{z}0} \end{bmatrix} \tag{20}$$

where $\mathbf{P}_0^+$ is the initial covariance matrix and the superscript '−' denotes the predicted variables.

The weights factors for the mean w_i^m and for covariance computation w_i^c are then initialized according to

$$\left.\begin{aligned} w_0^m &= \frac{(w_0-1)}{\alpha^2} + 1 \\ w_0^c &= \frac{(w_0-1)}{\alpha^2} + 2 + \beta - \alpha^2 \end{aligned}\right\}, \quad i = 0 \tag{21a}$$

$$w_i^m = w_i^c = \frac{w_i}{\alpha^2}, \quad i = 1, \ldots, p+1 \tag{21b}$$

where $w_i = (1 - w_0)/(p+1)$ and $0 \le w_0 \le 1$. The scaling parameter α determines the spread of the sigma points around $\hat{\mathbf{x}}_{k-1}^{\mathrm{a}+}$ and is usually set to a small positive value to minimize higher order effects ($10^{-4} \le \alpha \le 1$). The parameter β is used to make further higher order effects to be incorporated by adding the weighting of the 0th sigma point of the calculation of the covariance and it is minimized when $\beta = 2$ [17].

Next the sigma point set $\mathcal{X}_{k-1}^\mathrm{a}$ are generated, along with their associated weights factors, according to the desired selection scheme. For the spherical simplex scaled sigma points this give:

$$\mathcal{X}_{k-1}^\mathrm{a} = 0_{p\times(p+2)} \tag{22a}$$

$$\mathcal{X}_{(2:j+1),k-1}^\mathrm{a} = \frac{-1}{\sqrt{j(j+1)w_1}} \tag{22b}$$

$$\mathcal{X}_{j+2,k-1}^\mathrm{a} = \frac{j}{\sqrt{j(j+1)w_1}} \tag{22c}$$

$$\mathcal{X}_{i,k-1}^\mathrm{a} = \hat{\mathbf{x}}_{k-1}^{\mathrm{a}+} + \Delta\mathcal{X}_{i,k-1}^a \tag{22d}$$

with $\Delta\mathcal{X}^{a}_{i,k-1} \equiv \alpha\mathbf{S}^{\mathrm{a}}_{k-1}\mathcal{X}^{\mathrm{a}}_{i,k-1}$ and where $j = 1,\ldots,p$, w_i is the weights factors and $i = 1,\ldots,p+2$, indicates the ith scaled sigma point. The augmented system state square-root matrix $\mathbf{S}^{\mathrm{a}}_{k-1}$ can be obtained using lower triangular matrix of the Cholesky factorization such that

$$\mathbf{S}^{\mathrm{a}}_{k-1}\left(\mathbf{S}^{\mathrm{a}}_{k-1}\right)^{T} = \mathbf{P}^{\mathrm{a}}_{k-1} \tag{23}$$

where $\mathbf{P}^{\mathrm{a}}_{k-1}$ is positive definite or semidefinite matrix. Two efficient orthogonalization algorithms can be found in [22].

Note that the elements of $\Delta\mathcal{X}^{a}_{i,k-1}$ in Eq. (22d) are similar to the process noise $\eta_{\mathbf{x}k}$ of Eq. (18). If we interpret the sigma points as a set of disturbed state vectors, then Eq. (22d) describes how these disturbed state vectors are build from the set $\Delta\mathcal{X}^{a}_{i,k-1}$. However, the unit quaternion is not mathematically closed for addition and subtraction. The sigma points for the quaternion are also quaternions satisfying the normalization constraints and should be scattered around the current quaternion estimate on the unit sphere. Therefore, the quaternion sigma points are generated by multiplying the error quaternion by the current quaternion estimate. Then the set of $p+1$ scaled sigma points is split up and constructed as

$$\mathcal{X}^{\mathrm{a}}_{i,k-1} \equiv \begin{bmatrix} \mathcal{X}^{\mathbf{q}}_{i,k-1} \\ \mathcal{X}^{\mathrm{a}\backslash\mathbf{q}}_{i,k-1} \end{bmatrix} = \begin{bmatrix} \delta\mathbf{q}^{+}_{i,k-1} \otimes \hat{\mathbf{q}}^{+}_{k-1} \\ \hat{\mathbf{x}}^{\mathrm{a}\backslash\mathbf{q}+}_{k-1} + \Delta\mathcal{X}^{\mathrm{a}\backslash\mathbf{q}}_{i,k-1} \end{bmatrix} \tag{24}$$

where $\mathcal{X}^{\mathbf{q}}_{i,k-1}$ is the quaternion scaled sigma points corresponding to the quaternion attitude part, $\mathcal{X}^{\mathrm{a}\backslash\mathbf{q}}_{i,k-1}$ is the scaled sigma points corresponding to the rest part of the augmented state-vector and $\delta\mathbf{q}^{+}_{i,k-1}$ is the predicted error quaternion.

Since the role of process noise for the quaternion in Eq. (18) increases the uncertainty in attitude orientation, the process noise for the quaternion can be modeled as a rotation vector, that leading to orientation uncertainty in the attitude. Since the quaternion process noise is a 3-dimensional noise vector, it has to be expanded into a 4×1 dimensional unit quaternion to apply the multiplicative quaternion-error approach as follows

$$\delta\mathbf{q}^{+}_{i,k-1} = \begin{bmatrix} \dfrac{\sin\left\|0.5\phi_{i,k-1}\right\|}{\left\|0.5\phi_{i,k-1}\right\|}0.5\phi_{i,k-1} \\ \cos\left\|0.5\phi_{i,k-1}\right\| \end{bmatrix} \tag{25}$$

where $\phi_{i,k-1}$ is the rotation vector modeling the process noise for the quaternion.

During the prediction stage, the transformed spherical simplex scaled sigma point vectors are propagated through the system process model

$$\mathcal{X}^{-}_{i,k} = \mathbf{g}\left[t_k, \mathcal{X}^{\mathbf{x}}_{i,k-1}, \mathcal{X}^{\eta_{\mathbf{x}}}_{i,k-1}, \Delta\theta_k, \Delta\mathbf{v}^{b}_{\mathbf{f}k}\right] \tag{26}$$

where we have denoted the components of sigma points which correspond to actual state variables and process noise with matrices $\mathcal{X}^{\mathbf{x}}_{i,k-1}$ and $\mathcal{X}^{\eta_{\mathbf{x}}}_{i,k-1}$, respectively. The input vector $\mathbf{u}_k \equiv [\Delta\theta_k \ \Delta\mathbf{v}^{b}_{\mathbf{f}k}]$ is composed of the compensated outputs of the gyro and the accelerometer, respectively, defined in Eq. (16). The system process model $\mathbf{g}[\cdot]$ refer the overall INS navigation algorithm which is described in sections II.

Propagation stage is completed, the predicted state vector $\hat{\mathbf{x}}^{-}_{k}$ is calculated using a weighted sample mean of the propagated sigma points, $\mathcal{X}^{-}_{i,k}$, which is given by:

$$\hat{\mathbf{x}}^{-}_{k} = \sum_{i=0}^{p+1} w^{m}_{i}\mathcal{X}^{-}_{i,k} \tag{27}$$

However, the weighted sum of unit quaternions is generally not a quaternion of unit norm because the unit quaternion is not mathematically closed for addition and scalar multiplication. Therefore, the predicted attitude quaternion $\hat{\mathbf{q}}^{-}_{k}$ is determined as the barycentric mean with renormalization as follows

$$\hat{\mathbf{q}}^{-}_{k} = \frac{\hat{\mathbf{q}}^{-}_{k}}{\|\hat{\mathbf{q}}^{-}_{k}\|} \tag{28}$$

As in averaging attitude quaternions, the predicted covariance of posterior quaternions can not be directly computed because the unit quaternion is not closed for subtraction. We can use the quaternion-error for predicted covariance computation because it represents the distance from the predicted mean quaternion $\hat{\mathbf{q}}^{-}_{k}$. The quaternion-error for predicted covariance computation is given by

$$\delta\mathbf{q}^{-}_{i,k} = \mathcal{X}^{\mathbf{q}}_{i,k-1} \otimes (\hat{\mathbf{q}}^{-}_{k})^{-1} \tag{29}$$

Let denote $[\mathcal{X}^{-}_{i,k} - \hat{\mathbf{x}}^{-}_{k}]$ the difference between the sigma points and the predicted state vector as

$$\Delta\mathcal{X}^{-}_{i,k} \equiv \begin{bmatrix} \Delta\mathcal{X}^{\mathbf{q}-}_{i,k} \\ \Delta\mathcal{X}^{\mathbf{x}\backslash\mathbf{q}-}_{i,k} \end{bmatrix} \tag{30}$$

Since $\Delta\mathcal{X}^{\mathbf{q}-}_{i,k}$ is the predicted rotation vector corresponding to the quaternion-error $\delta\mathbf{q}^{-}_{i,k}$, *i.e* the rotation which turns the orientation part of $\hat{\mathbf{x}}^{-}_{k}$ into $\mathcal{X}^{-}_{i,k}$, the predicted covariance $\mathbf{P}^{-}_{k}$ can be then computed as

$$\mathbf{P}^{-}_{k} = \sum_{i=0}^{p+1} w^{c}_{i}[\Delta\mathcal{X}^{-}_{i,k}][\Delta\mathcal{X}^{-}_{i,k}]^{T} \tag{31}$$

In additive noise case the process noise is directly added to the state variables, but other forms of noise effect are now also allowed.

Once the predicted state and covariance are computed, the sigma points need to be regenerated using Eq. (24) in the update stage. Next, the sigma points are transformed through the measurement model:

$$\mathcal{Z}^{-}_{i,k} = \mathbf{h}\left[\mathcal{X}^{-}_{i,k}, \mathcal{X}^{\eta_{\mathbf{z}}}_{i,k-1}\right] \tag{32}$$

where we have denoted the component of sigma points corresponding to measurement noise with matrix $\mathcal{X}^{\eta_{\mathbf{z}}}_{i,k-1}$.

Similarly, the predicted measurement vector $\hat{\mathbf{z}}^{-}_{k}$ is also calculated as:

$$\hat{\mathbf{z}}^{-}_{k} = \sum_{i=0}^{p+1} w^{m}_{i}\mathcal{Z}^{-}_{i,k} \tag{33}$$

The predicted covariance of the measurement $\mathbf{P_{zz}}$ is given by

$$\mathbf{P_{zz}} = \sum_{i=0}^{p+1} w_i^c [\Delta\mathcal{Z}_{i,k}^-][\Delta\mathcal{Z}_{i,k}^-]^T \tag{34}$$

with $\Delta\mathcal{Z}_{i,k}^- = [\mathcal{Z}_{i,k}^- - \hat{\mathbf{z}}_k^-]$. The cross-covariance matrix of the state and measurements vectors $\mathbf{P_{xz}}$ is determinined using:

$$\mathbf{P_{xz}} = \sum_{i=0}^{p+1} w_i^c [\Delta\mathcal{X}_{i,k}^-][\Delta\mathcal{Z}_{i,k}^-]^T \tag{35}$$

The Kalman gain matrix $\mathbf{K}_k$ is then computed by:

$$\mathbf{K}_k = \mathbf{P_{xz}}\mathbf{P_{zz}^{-1}} \tag{36}$$

Finally, The estimated state vector $\hat{\mathbf{x}}_k^+$ and updated covariance $\mathbf{P}_k^+$ are given by

$$\hat{\mathbf{x}}_k^+ = \hat{\mathbf{x}}_k^- + \Delta\hat{\mathbf{x}}_k^+ \tag{37}$$

$$\mathbf{P}_k^+ = \mathbf{P}_k^- + \mathbf{K}_k\mathbf{P_{zz}}\mathbf{K}_k^T \tag{38}$$

with $\Delta\hat{\mathbf{x}}_k^+ \equiv [\Delta\hat{\mathbf{x}}_k^{\mathbf{q}+} \ \Delta\hat{\mathbf{x}}_k^{\mathbf{x}\backslash\mathbf{q}+}] = \mathbf{K}_k(\mathbf{z}_k - \hat{\mathbf{z}}_k^-)$ and where $\mathbf{z}_k$ is the measurement vector. However, the quaternion should be updated using quaternion multiplication. Then, the estimated quaternion $\hat{\mathbf{q}}_k^+$ is given by

$$\hat{\mathbf{q}}_k^+ = \delta\mathbf{q}_k^+ \otimes \hat{\mathbf{q}}_k^- \tag{39}$$

where $\delta\mathbf{q}_k^+$ is represented by

$$\delta\mathbf{q}_k^+ = \begin{bmatrix} \dfrac{\sin\left\|0.5\phi_k^+\right\|}{\left\|0.5\phi_k^+\right\|} 0.5\phi_k^+ \\ \cos\left\|0.5\phi_k^+\right\| \end{bmatrix}, \quad \phi_k^+ = \Delta\hat{\mathbf{x}}_k^{\mathbf{q}+} \tag{40}$$

IV. Numerical simulation and experimental results

The quaternion scaled unscented Kalman filter (Q-SUKF) developed in this paper is demonstrated using the experimental results in this section for a moving vehicle's attitude, position and velocity, as well as the initial sensors biases, scale factors. We assume that the misalignment errors of the initial sensors are considered equal to zeros in our case. The experimental platform consists of an INS aided by a GPS. The approach corresponds to a loosely integrated INS/GPS system. The experiment was conducted using an aircraft flying at a constant height for one hour. Its motion is described in NED coordinates with origin (point of interest) location at $\varphi_0 = 30$ deg and $\lambda_0 = -82$ deg. The initial velocity is given by $v_0^n = [0.5657 \ 0.5657 \ 0]^T$ m/s. We assume that the rotations about x-axis and y-axis are very small. The initial attitude is given by Euler angles $[\phi \ \theta \ \psi] = [0 \ 0 \ 0]$ degrees or by the quaternion $[\mathbf{q}_1 \ \mathbf{q}_2 \ \mathbf{q}_3 \ \mathbf{q}_4] = [0 \ 0 \ 0 \ 1]$. The gyro and accelerometer noises are given by their spectral densities $(3 \times 10^{-07})^2 I_{3\times3}$ rad/s$^{1/2}$ and $(10^{-04})^2 I_{3\times3}$ m/s$^{3/2}$, respectively. Since an INS integrates signals from accelerometers and gyroscopes, the white noise components are integrated and this will increase the uncertainty of the velocity and attitude. The gyro and accelerometer biases are considered as Random Walks and are given by their spectral densities $(10^{-06})^2 I_{3\times3}$ rad/s$^{3/2}$, $(5\times10^{-05})^2 I_{3\times3}$ m/s$^{5/2}$, respectively. Also, the gyro and accelerometer scale factor are modeled as Random Constants and are equals to $(0.01)I_{3\times3}$ and $(0.005)I_{3\times3}$, respectively. Initial biases for the gyros and accelerometers are given by 10 deg/hr and 0.003 m/s^2, respectively, for each axis. The GPS outages provide the position and velocity information in the WGS-84 reference with an accuracy of 1.5 m CEP and 0,03 m/s RMS, respectively. The sampling frequency of the GPS is 20 Hz, while the INS provides gyro and accelerometer data at 0.02 second intervals.

In general, velocity and position are very well known but attitude is not. To test the robustness of the Q-SUKF an initial attitude error of 60 degrees is given in each axis. The initial covariance matrix $\mathbf{P}_0$ in the Q-SUKF is diagonal. The diagonal terms of $\mathbf{P}_0$ represent variances or mean-squared errors. The off-diagonal terms are set to be zeros. For this case, the three attitude parts of the initial covariance are each set to a 3σ bound of 60 degrees, i.e., $[(60/3)\times\pi/180)]^2$ rad^2. The initial estimates for position are set to the true latitude, longitude and height. The initial variances for latitude and longitude are each given by $(1\times10^{-6})^2$ rad^2. The initial variance for height is given by $(10/3)^2$ m^2. The initial variances in the filters for v_N and v_E are each set to $(15/3)^2$ (m/sec)^2 and the initial variance for v_D is set to $(10/3)^2$ (m/sec)^2. The three gyro-bias parts of the initial covariance are each set to a 3σ bound of 30 degrees per hour, i.e., $[(30/3)\times\pi/(180\times3600))]^2$ (rad/sec)^2. The three accelerometer-bias parts of the initial covariance are each set to a 3σ bound of 0.005 meters per second-squared, i.e., $(0.005/3)^2$ rad^2/sec. The three gyro-scale factor parts of the initial covariance are each set to a 3σ bound of 0.015, i.e., $(0.015/3)^2$. Finally, the three accelerometer-scale factor parts of the initial covariance are each set to a 3σ bound of 0.010, i.e., $(0.010/3)^2$. The initial dynamic process noise is set as $\Sigma_{\mathbf{x}0}$, where the tuning of the diagonal terms of $\Sigma_{\mathbf{x}0}$ determines the performance of the filter. The initial measurement noise is $\Sigma_{\mathbf{y}0}$, where the diagonal terms of $\Sigma_{\mathbf{y}0}$ are initial measurement noises on INS and GPS velocity and position. The parameters used in the Q-SUKF developed are given by scaling parameters $\alpha = 0.05$ and $\beta = 2$, and by weight of 0th point $\omega_0 = 0.5$.

The quaternion errors are shown in Figure 1a. After 300 filter iterations which is approximately 150 seconds, the quaternion errors become very close to [0 0 0 1], which represents a zero rotation between the n-frame and the b-frame. Figure 1b show the attitude errors in the three axes and respective 3σ bounds (dashed lines in figures) derived from the Q-SUKF covariance matrix. All errors remain within their respective bounds, which indicates that the Q-SUKF is working properly. The tilt (roll and pitch) errors are less than ±0.5 degrees. The heading (yaw) errors are within ±2.5 degrees. The larger errors in heading are due to the fact that this angle is the least observable state for the particular vehicle motion. Figure 2a shows that all position errors remain inside their respective 3σ bounds, i.e., within 1×10^{-4} degrees for latitude and longitude, and within 1.5 meters for the height.

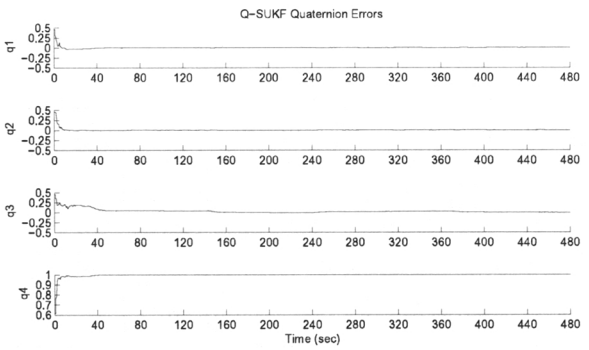

(a) Quaternion errors

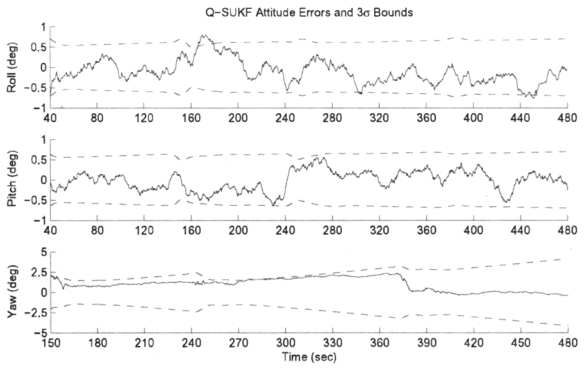

(b) Attitude errors are expressed in terms of Euler angles.

Figure 1. The 3σ bounds for the errors in Attitude

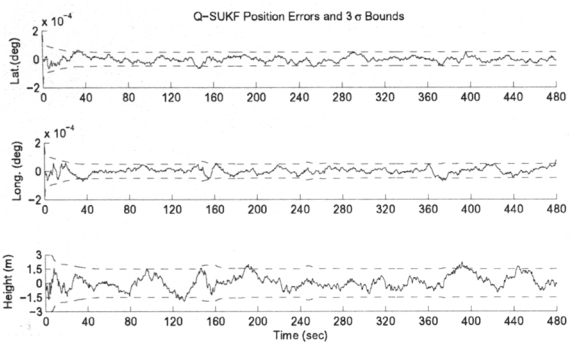

(a) Position errors in the three axes.

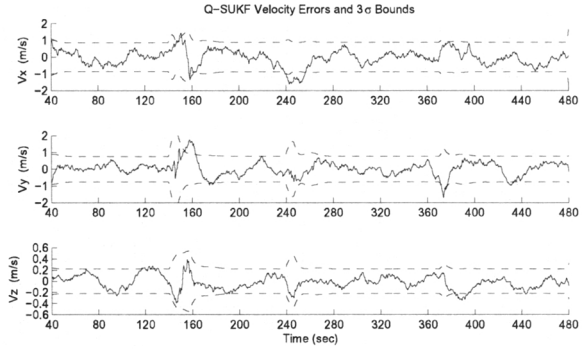

(b) Velocity errors in the three axes.

Figure 2. The 3σ bounds for the errors in Velocity and Position

Figure 2b shows the relative velocity errors, which shows that velocity errors in axes x and y are within 1 meters per second and in axis z is less than 0.2 meters per second for the vertical component. These simulation results indicate that the developed Q-SUKF algorithm is able to provide robust characteristics for integrating inertial navigation with GPS velocity/position measurements under large attitude error conditions.

V. Conclusion

Since the behavior and the accuracy of an INS navigation algorithm are strongly influenced by INS errors, this paper develops an integrating Inertial Navigation aided by GPS measurements for large attitude errors using quaternion parameterization of the attitude, velocity and position. Differing from other quaternion models, the weighted mean computation for quaternions is derived in rotational space as a barycentric mean with renormalization and a multiplicative quaternion-error is used for predicted covariance computation of the quaternion because it represents the distance from the predicted mean quaternion. The updates are performed using quaternion multiplication which guarantees that quaternion normalization is maintained in the filter. Since the quaternion process noise resulted in increase of the uncertainty in attitude orientation, it is modeled as a rotation vector. Numerical simulation results showed that attitude, velocity and position accuracy can be achieved using the proposed approach for large attitude errors.

References

[1] M. S. Grewal, L. R. Weill, and A. P. Andrews, *Global Positioning Systems, Inertial Navigation, and Integration.* John Wiley & Sons, Inc., 2001.

[2] R. M. Rogers, *Applied Mathematics in Integrated Navigation Systems.*, 2nd ed. Reston, Virginia: AIAA Education Series, 2003.

[3] O. Salychev, *Applied Inertial Navigation: Problems and Solutions.* Moscow, Russia: BMSTU Press, 2004.

[4] D. H. Titterton and J. L. Weston, *Strapdown Inertial Navigation Technology.*, 2nd ed. Reston, Virginia: AIAA Education Series, 2004, vol. 207.

[5] X. Kong, "INS algorithm using quaternion model for low cost IMU." *Robotics and Autonomous Systems*, vol. 46, no. 4, pp. 221–246, 2004.

[6] E.-H. Shin, "Estimation Techniques for Low-Cost Inertial Navigation," UCGE Reports Number 20219, The University of Calgary, Calgary, Alberta, Canada, May 2005.

[7] J. L. Crassidis, "Sigma-point kalman filtering for intagrated GPS and inertial navigation." *IEEE Transactions on Aerospace and Electronic Systems*, vol. 42, no. 2, pp. 750–756, 2006.

[8] M. D. Shuster, "A survey of attitude representationss." *Journal of the Astronautical Sciences*, vol. 41, no. 4, pp. 439–517, 1993.

[9] J. L. Crassidis and F. L. Markley, "Unscented filtering for spacecraft attitude estimation." *Journal of Guidance, Control, and Dynamics*, vol. 26, no. 4, pp. 536–542, 2003.

[10] F. L. Markley, "Attitude error representations for kalman filtering." *Journal of Guidance, Control, and Dynamics*, vol. 26, no. 2, pp. 311–317, 2003.

[11] R. B. Miller, "A new strapdown attitude algorithm." *Journal of Guidance and Control*, vol. 6, no. 4, pp. 287–291, 1983.

[12] J. Waldmann, "Attitude determination algorithms, computational complexity, and the accuracy of terrestrial navigation with strapdown inertial sensors." in *XIV Congress Brasileiro de Automatica*, 2002, pp. 2367–2373.

[13] J. R. Wertz, Ed., *Spacecraft Attitude Determination and Control.* Dordrecht, Holland: D. Reidel Publishing Company, 1984.

[14] P. G. Savage, "Strapdown inertial navigation integration algorithm design part 1: Attitude algorithms." *Journal of Guidance, Control, and Dynamics*, vol. 21, no. 1, pp. 19–28, 1998.

[15] ——, "Strapdown inertial navigation integration algorithm design part 2: Velocity and position algorithms." *Journal of Guidance, Control, and Dynamics*, vol. 21, no. 2, pp. 208–221, 1998.

[16] S. J. Julier and J. K. Uhlmann, "A new extension of the kalman filter to nonlinear systems." in *Proceedings of AeroSense: 11th Int. Symp. Aerospace/Defense Sensing, Simulation and Controls*, 1997, pp. 182–193.

[17] E. A. Wan and R. van der Merwe, *Kalman Filtering and Neural Networks*, H. S., Ed. New York: John Wiley & Sons, 2001.

[18] S. J. Julier and J. K. Uhlmann, "Reduced sigma point filters for the propagation of means and covariances through nonlinear transformations." in *Proceedings of the IEEE*, vol. 92(3), 2004, pp. 401–422.

[19] S. J. Julier, J. K. Uhlmann, and H. F. Durrant-Whyte, "A new method for the nonlinear transformation of means and covariances in filters and estimators." *IEEE Transactions on Automatic Control*, vol. 45, no. 3, pp. 477–482, 2000.

[20] S. J. Julier, "The scaled unscented transformation." in *Proceedings of the IEEE American Control Conference*, Evanston IL, USA, 2002, pp. 1108–111.

[21] ——, "The spherical simplex unscented transformation." in *Proceedings of the IEEE American Control Conference*, vol. 3, Denver CO, USA, 2003, pp. 2430–2434.

[22] H. Golub and C. van Loan, *Matrix Computations.*, 3rd ed. The JHU Press, 1996.